ELSEVIER

Physica B 297 (2001) 40–44

PHYSICA B

www.elsevier.com/locate/physb

Dynamics of PVA-gel with magnetic macrojunctions

Gy. Török[a,*], V.T. Lebedev[b], L. Cser[a], Gy. Káli[c], M. Zrinyi[d]

[a]*Research Institute for Solid State Physics, Konkoly, Th.u. 29-33, P.O.B 49, H-1525, Budapest XII, Hungary*
[b]*Petersburg Nuclear Physics Institute, 188300, Gatchina, Russia*
[c]*Hahn-Meitner Institut Berlin, Glienicker str 100, Berlin D-14109, Germany*
[d]*Technical University of Budapest, H-1521, Budapest, Hungary*

Abstract

The neutron-spin-echo spectrometer SPAN [C. Pappas et al., Physica B 276–278 (2000) 162] has been used for the study of the dynamics of ferrogel of Poly(vinylalcohol) with subdomain particles of magnetite (size ~ 10 nm, concentration in gel $C = 4.25$ wt%.) embedded in polymer matrix. By separation of coherent nuclear scattering on particles from incoherent one, contributed by network and solvent, we distinguished the dynamical behaviours of subsystems in ferrogel. The self-correlation of magnetic particle, attached to network, via its conformational changes obeys the law: $S_p(q,t) \sim \exp\{-q^2a^2[1-\cos(2\pi(t/\tau)^\beta)]/2\}$ where the $a \sim 1$ nm is the amplitude of particle's oscillation, and the exponent $\beta \sim \frac{1}{2}$ characterises the rotational diffusion of chain units with relaxation time $\tau \sim 0.3$ ns. In the surrounding solvent, half of the molecules showed free diffusion whereas the remaining part, situated in the neighbourhood of polymer chains, is involved in the stretched relaxation.

Keywords: Ferrogel; Neutron spin echo; Incoherent scattering

1. Introduction

Ferrogels belong to new nanophase materials [1,2], having specific features arising from the combination of polymer and dispersed magnetic phase (giant magneto–elastic effect [1]). The understanding as well as the improvement of their properties needs the extended investigations of ferrogel structures and dynamics of polymer and magnetic subsystem. Among these compounds the gel of Poly(vinylalcohol) (PVA) with subdomain magnetite particles exhibits an anomalous behaviour in the nanosecond range [3], related to the dynamic interaction of magnetic component and polymer network, that is studied in this paper.

In PVA-ferrogel [1,3] the magnetic particles, attached to the network (~ 300 monomer units between junctions), serve as microprobes. It enabled us to examine the slow chain dynamics induced by thermal motion of massive particles having the momentum $P \sim (3kTm)^{1/2}$. Note, the momentum of a particle outweighs by an order the momentum of chain unit. Thus, one can study separately a low-frequency relaxation mode in polymer network (coherent component). Particles playing the role of macrojunctions [2,3], have a good contrast in protonated matrix. This approach seems to be effective when we deal with a wide relaxation spectrum of polymer network. On the other hand, the

* Corresponding author. Tel.: +36-1-169-9499; fax: +36-1-3959165.

E-mail address: torok@power.szfki.kfki.hu (G. Török).

0921-4526/01/$ - see front matter
PII: S0921-4526(00)00868-1

incoherent part of scattering (from polymer and water) exhibits the dynamics of chain units and coupled solvent molecules.

2. Experiment

Dynamics of ferrogel, composed of magnetite particles (~ 10 nm) associated with PVA-network allowed to swell in water has been studied using neutron spin echo (NSE). The measurements were carried out in the momentum transfer $q = 0.24$–$1.5\ \mathrm{nm}^{-1}$ and time range $t = 0.01$–2.2 ns at the temperature $T = 343$ K without applied field.

The NSE-spectrometer SPAN [4] has a novel magnetic field configuration, which optimises the conditions for multidetector NSE. The precession field is created by the three pairs of coils with diameters of 1,3 and 4.8 m. Each pair is mounted in a Helmholtz-like fashion, one coil above and one coil below the scattering plane. The set-up has a symmetry axis, which is vertical and crosses the sample position. The magnetic field is therefore the same for all scattering angles and thus fulfills the condition for simultaneous NSE-measurements over a wide angular range. The maximum magnetic field integral is of $0.06Tm$ typically $\sim \frac{1}{3}$ that of IN11. The present NSE configuration covers that of energy transfer 300 μeV $\geqslant \hbar\omega \geqslant \frac{1}{\mathring{}}$ μeV at 3.8 $\mathring{A}$, and 24 μeV $\geqslant \hbar\omega \geqslant 80$ neV at 9 $\mathring{A}$, respectively. The main precession magnetic field is created by the coils with a diameter of 3 m, which have the electric currents antiparallel to each other. The resulting magnetic field at the scattering plane is horizontal with the required axial symmetry but becomes zero at the sample position. The coils with a diameter of 1 m shape the magnetic field around the sample. They produce at the sample a weak and homogeneous vertical field, which assures the axial symmetry of the magnetic configuration. The coils with a diameter of 4.8 m shape the axial component of the magnetic field at the position of the $\pi/2$ flippers. Remanent supermirrors produced at the PSI, which perform in the stray magnetic field of the main precession coils and require no additional magnetic field, are used as analysers. Presently, 10 detectors are equipped with analysers with an opening of 8°. The NSE measurements with the installed correction coils (fresnels, linear shifter) allowed to use the total vertical beam divergence of 1.2° FWHM, which led to the expected high data acquisition rate. SPAN is now in routine operation at BENSC. It is designed to be a versatile and flexible instrument.

In NSE-experiments we observed both inelastic nuclear coherent and incoherent scattering. A weak magnetic component, being of order of $\sim 1\%$ of nuclear one, does not contribute to NSE-signal because the paramagnetic scattering gives the polarisation $\boldsymbol{P}_m = -\boldsymbol{e}(\boldsymbol{e}\boldsymbol{P}_0) = 0$ at the unit scattering vector $\boldsymbol{e} \perp \boldsymbol{P}_0$ ($\boldsymbol{P}_0$ is the initial polarisation at the sample). Therefore there is no NSE-focusing for weak paramagnetic component. Thus, our data are treated in terms of coherent scattering (from particles) and incoherent one (from water and network). The polymer content in gel is ~ 6.3 wt% that is the incoherent scattering from water dominates. The NSE-signal can be written in the following form:

$$P_{\mathrm{nse}}(q,t) = \frac{I_{\mathrm{coh}} S_{\mathrm{coh}}(q,t) + P_{\mathrm{inc}} I_{\mathrm{inc}} S_{\mathrm{inc}}(q,t)}{I_{\mathrm{coh}} + P_{\mathrm{inc}} I_{\mathrm{inc}}}, \tag{1}$$

where $I_{\mathrm{coh}}, S_{\mathrm{coh}}(q,t)$ represent the measured coherent intensity and scattering function, I_{inc}, $S_{\mathrm{inc}}(q,t)$ are similar terms related to incoherent scattering and the polarisation normalised to P_0 is about $P_{\mathrm{inc}} \approx -0.25 > -\frac{1}{3}$. The deviation from the value $-\frac{1}{3}$ can be explained by the effect of multiple scattering. From the polarisation measurement one can derive these two components shown in Fig. 1:

$$I_{\mathrm{coh}}(q) = \frac{I_t(P_t/P_0 - P_{\mathrm{inc}})}{(1 - P_{\mathrm{inc}})},$$

$$I_{\mathrm{inc}}(q) = \frac{I_t(1 - P_t/P_0)}{(1 - P_{\mathrm{inc}})}. \tag{2}$$

The sum $I_{\mathrm{t}} = I_{\mathrm{coh}} + I_{\mathrm{inc}}$ is the total scattered intensity and P_{t} is the polarisation, normalised to its initial magnitude $P_0 = 0.9$. The incoherent component remains practically constant over the q-range of observation, whereas the coherent component being larger than incoherent background at low q decreases with momentum transfer and follows the scattering law: $I_{\mathrm{coh}}(q) = I_0/[1 + (R_{\mathrm{c}}q)^2]^2$. The correlation radius of a particle is $R_{\mathrm{c}} \sim 6$ nm

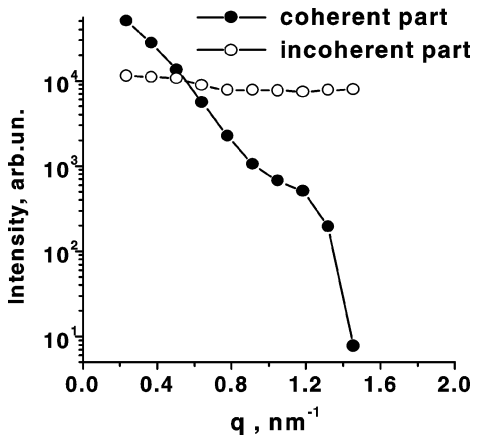

Fig. 1. Coherent and incoherent intensities versus momentum transfer.

that gives the value of its diameter $D_p \sim 18$ nm. Then we determined the amplitude of the NSE-signal, $A = |[I_{coh}S_{coh}(q,t) + P_{inc}I_{inc}S_{inc}(q,t)]|$ normalised to the corresponding difference of intensities $I_{coh} + P_{inc}I_{inc}$. This term is positive at low q and negative when incoherent scattering dominates. Therefore, we observed that the NSE-signal changes from positive to negative magnitude in the experimental q-range (Fig. 2).

3. Discussion

The NSE-signal at the lowest q (Fig. 2) is determined by the dynamics of particles attached to network and playing the role of macrojunctions. The contribution of incoherent scattering of water and that of the network is negligible compared to the total intensity, $I_{inc}/I_{coh} < 0.2$. In addition, the water diffusion is relatively slow at this time-scale. Of course, one can estimate the change of autocorrelation function by water diffusion as $S_w(q,t) = \exp(-D_w q^2 t_{max}) \sim 0.95$ at maximum time $t_{max} \sim 2.2$ ns and $q \sim 0.3$ nm^{-1} for known diffusion coefficient at 70°C, $D_w \sim 6 \times 10^{-5}$ cm^2/s^{-1}. At higher $q \sim 0.6$ nm^{-1} the coherent components becomes smaller than the incoherent one, $I_{coh}/I_{inc} \sim 0.6$. So the water dynamics gives a negative contribution to NSE-signal. The last comes up with time increasing. At higher q the diffusive water dynamic drastically diminishes even at very small times ($t < 0.2$ ns). The "residual" NSE-signal shows an oscillating behaviour to be treated as the motion of water together with the network with moving particles associated.

We succeeded in separating the coherent scattering function at low q from the incoherent one, using the known incoherent intensity and autocorrelation function of water $S_w(q,t) = \exp(-D_w q^2 t)$. At intermediate and high q we extracted the incoherent scattering function, subtracting the small coherent part from the NSE-signal. The experimental results were fitted with autocorrelation function

$$S(q,t) = \exp\left[\frac{-q^2\langle\Delta X^2(t)\rangle}{2}\right]. \quad (3)$$

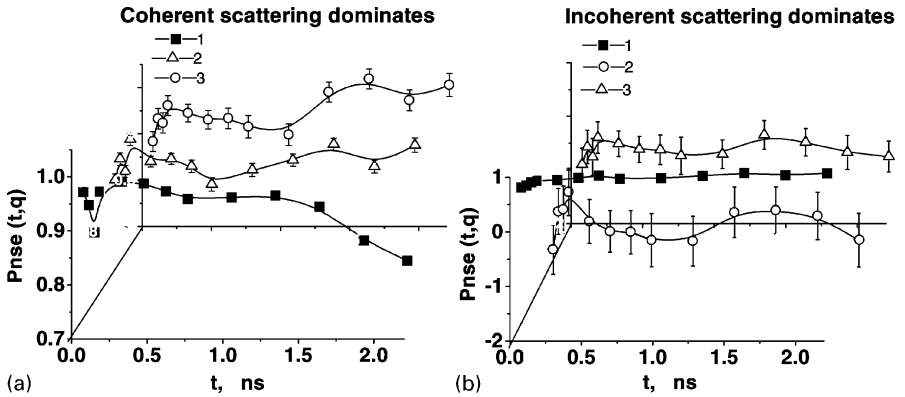

Fig. 2. NSE-signal at different momentum transfer: (a) $q = 0.24$ nm^{-1} (1); 0.37 nm^{-1} (2); 0.51 nm^{-1} (3); (b) $q = 0.64$ nm^{-1} (1); 1.32 nm^{-1} (2); 1.46 nm^{-1} (3). Lines are a guide to the eye.

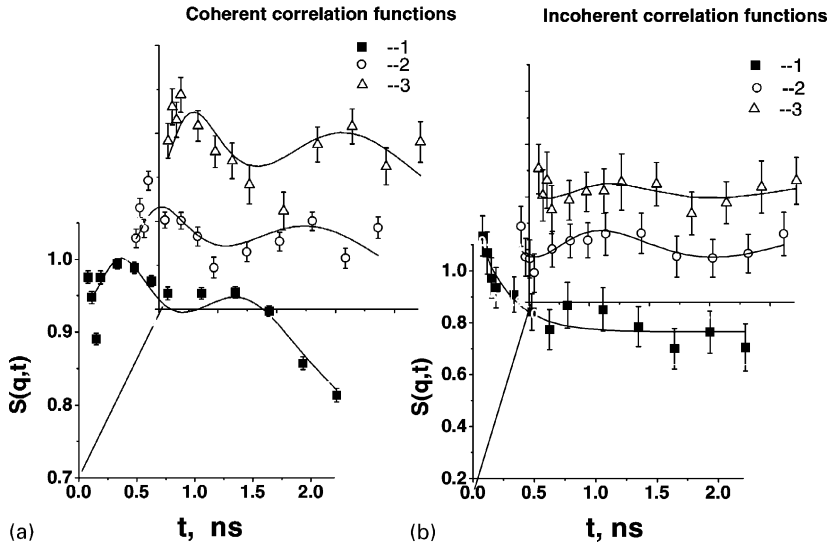

Fig. 3. The coherent and incoherent dynamic scattering functions at different q: (a) $q = 0.24\ \mathrm{nm}^{-1}$ (1); $0.37\ \mathrm{nm}^{-1}$ (2); $0.51\ \mathrm{nm}^{-1}$ (3); (b) $q = 0.64\ \mathrm{nm}^{-1}$ (1); $1.32\ \mathrm{nm}^{-1}$ (2); $1.46\ \mathrm{nm}^{-1}$ (3). Solid lines represent the fitting functions.

The results of the approximation are shown in Fig. 3. As usual, the averaged squared shift of a particle $\langle \Delta X^2(t) \rangle$ along $\boldsymbol{q}$ can be evaluated as a sum of oscillating (localized) and translational components statistically independent: $\langle \Delta X^2(t) \rangle = \langle \Delta X^2(t)_{\mathrm{O}} \rangle + \langle \Delta X^2(t)_{\mathrm{T}} \rangle$. At initial state of diffusion particle is moving with velocity $\langle v^2 \rangle \sim kT/m$ (m is the mass of a particle) that gives the squared shift $\langle \Delta X^2(t)_{\mathrm{T}} \rangle = \langle v^2 \rangle t^2$. The vibrations of a particle in the network, $X(t) = a\cos(\varphi(t))$, with amplitude a and phase $\varphi(t)$ can be described by the equation

$$\frac{\mu\, \mathrm{d}X(\varphi)}{\mathrm{d}t} + K(t)X(\varphi - \varphi^*) = 0. \tag{4}$$

Here we took into account the high viscosity of polymer medium (μ is the friction coefficient of a particle), the function of the relaxation of chain modulus, $K(t)$, created by the conformational changes in polymer and the delayed response of polymer on local chain perturbation (phase shift φ^*). As it is known [5], the shift modulus of entangled system of chains under applied force decreases as $K(t) = K_{\mathrm{E}}(\tau_{\mathrm{E}}/t)^{1/2}$ (K_{E} is the value of modulus at characteristic time $t = \tau_{\mathrm{E}}$). Thus, we obtain the oscillating solutions with phase $\varphi_m = \Omega_m t^{1/2}$ at the condition $\cos(\varphi_m^*) = 0$, i.e. $\varphi^* = \varphi(\tau^*) = \Omega_m \tau^{*1/2} = \pi(2m + 1)/2$ where $m = 0,1,2\ldots$. So the "frequencies" $\Omega_m = (2K_{\mathrm{E}}\tau_{\mathrm{E}}^{1/2}/\mu) = \Omega_0(2m + 1)$ are dependent on characteristic time τ^* and the lowest frequency $\Omega_0 = \pi/2\tau^{*1/2}$. This delay time $\tau^* \sim s/c$, should be of order of the time of torsion wave propagation (velocity c) between network junctions (chain fragment of length s). Using the solution $X(t) = a\cos(\varphi(t))$ one can evaluate the squared shift $\langle \Delta X^2(t)_{\mathrm{O}} \rangle = a^2[1 - \cos[2\pi(t/\tau)^{\beta}]]$ where the exponent $\beta = \frac{1}{2}$ and the period $\tau = (2\pi/\Omega)^{1/\beta}$. We have used it in data treatment to find the amplitude a, periods τ and stretching parameter β for coherent scattering at low q (Table 1). For water diffusion at intermediate q we have taken the shift $\langle \Delta X^2(t) \rangle = 2D_{\mathrm{w}}t$, depending on the diffusion constant D_{w}. At large q we again applied the approach of stretched oscillation with parameters corresponding to slow dynamics of water attached to network: $\Delta X_{\mathrm{w}}^2(t) = a_{\mathrm{w}}^2[1 - \cos[2\pi(t/\tau_{\mathrm{w}})^{\beta}]]$. These fitting functions describe the data satisfactorily (Fig. 3) at the following parameters:

The behaviours of coherent and incoherent scattering functions are quite similar that is described by stretching parameter $\beta \sim 0.4$–0.5. The particles are moving with higher amplitude and shorter period (both factors two) as compared to surrounding gel. The low-q measurement gives the thermal

Table 1
Dynamic parameters

$S(q,t)$	q (nm^{-1})	a (nm)	τ (ns)	β	v ($cm\ s^{-1}$)
Coherent	0.24	1.04 ± 0.19	0.37 ± 0.03	0.5	103 ± 19
Coherent	0.37	0.59 ± 0.16	0.30 ± 0.04	0.4	38 ± 12
Coherent	0.51	0.50 ± 0.13	0.29 ± 0.04	0.4	29 ± 11
Incoherent	1.32	0.30 ± 0.05	0.73 ± 0.07	0.5	—
Incoherent	1.46	0.21 ± 0.07	0.68 ± 0.13	0.5	—

velocity of a particle whereas at higher q we have magnitudes contaminated by other processes (particles' rotations). This dynamic behaviour is connected with network parameters. The size of this network cell ($\xi \sim 8$ nm) is estimated from concentration of junctions (one junction per 600 units, i.e. 300 units between junctions). Taking these amplitudes we obtained the frequency of oscillation for a particle confined in the network whose junctions are attached to particles' surface: $\omega \sim [(2kT/a^2)\ 16\pi R_p^2/\xi^2 m)]^{1/2} \sim 0.6 \times 10^{10}\ s^{-1}$ where the radius of a particle $R_p \sim 9$ nm, the amplitude of oscillations $a \sim 1$ nm and the temperature $T = 343$ K. This rough estimation gives the same order as experimental frequency $\omega_{coh} = 2\pi/\tau_{coh} = 1.6 \times 10^{10}\,s^{-1}$ for particles oscillations and it is close to the observed frequency in gel: $\omega_{inc} = 2\pi/\tau_{inc} = 0.8 \times 10^{10}\ s^{-1}$. As we found, $\sim 70\%$ of water molecules are associated to network; this is evident from scattering function behaviour. The free molecules exhibit fast diffusion with constant $D_w = (9.4 \pm 3.0)10^{-5}\ cm^2\ s^{-1}$ corresponding to pure water diffusion rate.

Acknowledgements

The authors are grateful to Drs. I.N. Ivanova and S.M. Bogdanovich for assistance. This work was supported by the Russian Ministry of Science and Technology (prg. "Uporyadochenie", "Neutron Res. of Condensed Matter"), Russian Fund for basic Research (Grant L-EN-96-15-96775). The experiments at BENSC were supported by European Commission through TMR programme "Access to large scale facilities" ERB FMGECT 950060.

References

[1] M. Zrinyi, L. Barsi, A. Buki, J. Chem. Phys. 104 (1996) 8750.
[2] Gy. Török, V.T. Lebedev, L. Cser, A.L. Buyanov, L.G. Revelskaya, Physica B 276–278 (2000) 398.
[3] Gy. Török, V.T. Lebedev, L. Cser, M. Zrinyi, Physica B 276–278 (2000) 396.
[4] C. Pappas, G. Káli, P. Böni, R. Kischnik, L.A. Mertens, P. Granz, F. Mezei, Physica B 276–278 (2000) 162.
[5] A.Yu. Grosberg, A.R. Khokhlov, Statistical Mechanics of Macromolecules, Nauka, Moscow, 1989, p. 281.